

Volume Dependence of Bound States with Angular Momentum

Sebastian König,¹ Dean Lee,^{2,1} and H.-W. Hammer¹

¹*Helmholtz-Institut für Strahlen- und Kernphysik (Theorie)
and Bethe Center for Theoretical Physics, Universität Bonn, 53115 Bonn, Germany*

²*Department of Physics, North Carolina State University, Raleigh, NC 27695, USA*

(Dated: January 15, 2013)

We derive general results for the mass shift of bound states with angular momentum $\ell \geq 1$ in a finite periodic volume. Our results have direct applications to lattice simulations of hadronic molecules as well as atomic nuclei. While the binding of S-wave bound states increases at finite volume, we show that the binding of P-wave bound states decreases. The mass shift for D-wave bound states as well as higher partial waves depends on the representation of the cubic rotation group. Nevertheless, the multiplet-averaged mass shift for any angular momentum ℓ can be expressed in a simple form, and the sign of the shift alternates for even and odd ℓ . We verify our analytical results with explicit numerical calculations. We also show numerically that similar volume corrections appear in three-body bound states.

PACS numbers: 12.38.Gc, 03.65.Ge, 21.10.Dr

Introduction. With recent advances in computational power and algorithms, the physics of numerous quantum few- and many-body systems can now be investigated from first principles. Lattice simulations are an important tool for such calculations [1–3]. The system is solved numerically using a discretized spacetime in a finite volume. In practice, the finite volume is usually a cubic box with periodic boundaries. The box modifies the bound state wave functions and leads to shifts in the binding energies. This shift needs to be subtracted from the calculated energies for comparison to experiment. In the case of S-wave bound states, Lüscher has derived a formula for the finite volume mass shift of two-body states [4]. See Ref. [5] for a recent application of this method in lattice QCD to extract the mass of the proposed H-dibaryon.

But there are also many bound states with nonzero orbital angular momentum. In nuclear physics, some particularly interesting examples occur in halo nuclei [6–9]. These nuclei show a pronounced cluster structure. One-neutron halo nuclei can be regarded as a tightly-bound core with an extra neutron. In such cases the separation energy for the neutron is much smaller than the binding energy of the core as well as the energy required for core excitation. Thus, the volume dependence of energy levels obtained in *ab initio* lattice calculations of such halo systems would behave as a two-body system.

A well known example of a P-wave halo state is the $J^P = 1/2^-$ excited state in ^{11}Be . The electromagnetic properties of the low-lying states in ^{11}Be can be well described in a two-body halo picture [7, 9]. If Coulomb interactions are included, proton halos like ^8B also become accessible. In atomic physics, several experiments have investigated strongly-interacting P-wave Feshbach resonances in ^6Li and ^{40}K [10–12] which can be tuned to produce bound P-wave dimers. There is interest in P-wave molecules in hadronic physics [13] as well as lattice investigations of the excited nucleon spectrum in a

number of different spin channels [14]. Some of these states have been conjectured to have a molecular baryon-meson structure [15]. An extension of Lüscher’s formula to higher partial waves would provide a tool to discern molecular structures in hadronic states as well as halo structures in nuclei from the finite-volume dependence of lattice calculations for such systems.

In this letter, we derive general formulas for the finite-volume mass shift for bound states with nonzero orbital angular momentum ℓ . We also obtain a simple expression for the multiplet-averaged mass shift for angular momentum ℓ . We verify our analytical results with numerical calculations using an attractive short-range potential. We note recent studies on the related topics of extracting resonance properties and scattering phase shifts in higher partial waves from finite-volume energy levels [16, 17]. Although our analytic derivation can be applied rigorously only to two-body systems, we show numerically that quantitatively similar results also appear in three-body systems.

Mass shift formula. In order to derive a general mass shift formula we consider a bound state solution $|\psi_B\rangle$ of the Schrödinger equation

$$\hat{H} |\psi_B\rangle = -E_B |\psi_B\rangle, \quad \hat{H} = -\frac{1}{2\mu} \Delta_r + V(\mathbf{r}) \quad (1)$$

with angular quantum numbers (ℓ, m) in a finite box of size L^3 with periodic boundary conditions. Following Lüscher’s derivation in [4], the energy shift compared to the infinite volume solution,

$$\Delta m_B = E_B(\infty) - E_B(L), \quad (2)$$

can be written as

$$\Delta m_B^{(\ell, m)} = \sum_{|\mathbf{n}|=1} \int d^3r \psi_B^*(\mathbf{r}) V(\mathbf{r}) \psi_B(\mathbf{r} + \mathbf{n}L) + \mathcal{O}(e^{-\sqrt{2}\kappa L}), \quad (3)$$

where \mathbf{n} is an integer vector and $\kappa \equiv \sqrt{2\mu E_B}$ is the binding momentum. We assume that the potential has a finite range $R \ll L$. Eq. (3) arises from the overlap between copies of the system introduced by the periodic boundary conditions. For $r > R$, the wave function has the asymptotic form

$$\psi_B(\mathbf{r}) = Y_\ell^m(\theta, \phi) \frac{i^\ell \gamma \hat{h}_\ell^+(i\kappa r)}{r}, \quad \gamma \in \mathbb{R}, \quad (4)$$

where \hat{h}_ℓ^+ is a Riccati–Hankel function. We will use the relation

$$Y_\ell^m(\theta, \phi) \frac{\hat{h}_\ell^+(i\kappa r)}{r} = (-i)^\ell R_\ell^m \left(-\frac{1}{\kappa} \nabla_r \right) \left[\frac{e^{-\kappa r}}{r} \right], \quad (5)$$

which follows from Lemma B.1 in [18] and a derivative formula for spherical Hankel functions [19]. The functions R_ℓ^m are the solid harmonics defined via $R_\ell^m(\mathbf{r}) = r^\ell Y_\ell^m(\theta, \phi)$.

For S-waves, Eq. (5) is a trivial identity. Inserting the Schrödinger equation to rewrite $V(\mathbf{r})$ in (3), and using the fact that $\exp(-\kappa r)/(4\pi r)$ is a Green’s function for the operator $[\Delta_r - \kappa^2]$, we recover Lüscher’s result for S-wave bound states. In our notation this reads

$$\Delta m_B = -3|\gamma|^2 \frac{e^{-\kappa L}}{\mu L} + \mathcal{O}(e^{-\sqrt{2}\kappa L}). \quad (6)$$

We now generalize the mass shift formula to higher orbital angular momentum. In the following we explicitly show the derivation for P-waves. We insert the asymptotic expression (4) with $\ell = 1$ into Eq. (3) and use (5) to rewrite the Riccati–Hankel function. For $m = 0$ we find

$$\Delta m_B^{(1,0)} = -\frac{\sqrt{3}\pi\gamma}{\mu\kappa} \sum_{|\mathbf{n}|=1} \frac{\partial}{\partial z} \psi_B^*(\mathbf{r} - \mathbf{n}L) \Big|_{\mathbf{r}=0} + \mathcal{O}(e^{-\sqrt{2}\kappa L}) \quad (7)$$

after integrating by parts. For $m = \pm 1$, the result is similar and involves derivatives with respect to x and y . Evaluating the sums then yields

$$\Delta m_B^{(1,0)} = \Delta m_B^{(1,\pm 1)} = 3|\gamma|^2 \frac{e^{-\kappa L}}{\mu L} + \mathcal{O}(e^{-\sqrt{2}\kappa L}). \quad (8)$$

Compared to the S-wave case, the P-wave mass shift is opposite in sign but equal in magnitude. Qualitatively, this means that S-wave bound states are more deeply bound when put in a finite volume while P-wave states are less bound.

For higher partial waves we can proceed in exactly the same manner. The results, however, are more complicated and the shift for D-waves and higher partial waves depends on the quantum number m . We note that due to the periodic boundaries, the rotational symmetry group

is reduced to a cubic subgroup. As a consequence, angular momentum multiplets are split into irreducible representations of this subgroup (see, for example, Ref. [16]). A similar splitting also arises in lattice calculations due to discretization artifacts.

The mass shift for general ℓ can be expressed as

$$\Delta m_B = \alpha\left(\frac{1}{\kappa L}\right) \cdot |\gamma|^2 \frac{e^{-\kappa L}}{\mu L} + \mathcal{O}(e^{-\sqrt{2}\kappa L}), \quad (9)$$

where the coefficients $\alpha\left(\frac{1}{\kappa L}\right)$ are given in Tab. I for $\ell = 0, 1, 2$. The irreducible representation of the cubic group is denoted by Γ in Tab. I. A detailed derivation of the general mass shift formula will be provided in a forthcoming publication [20]. The expressions for the fi-

ℓ	Γ	$\alpha(x)$
0	A_1^+	-3
1	T_1^-	+3
2	T_2^+	$30x + 135x^2 + 315x^3 + 315x^4$
2	E^+	$-1/2 (15 + 90x + 405x^2 + 945x^3 + 945x^4)$

TABLE I: Coefficient $\alpha(x)$ in the expression for the finite volume mass shifts for $\ell = 0, 1, 2$. Γ indicates the corresponding representation of the cubic group.

nite volume mass shift become simpler when we sum over all m for a given ℓ . Using the trace formula for spherical harmonics, it can be shown [20] that

$$\sum_{m=-\ell}^{\ell} \Delta m_B^{(\ell,m)} = (-1)^{\ell+1} (2\ell+1) \cdot 3|\gamma|^2 \frac{e^{-\kappa L}}{\mu L} + \mathcal{O}(e^{-\sqrt{2}\kappa L}). \quad (10)$$

Dividing by $2\ell+1$, we obtain the average mass shift for states with angular momentum ℓ . Apart from the overall sign, this average shift is independent of ℓ . This follows from the fact that $Y_\ell^m(\theta, \phi) Y_\ell^{m*}(\theta, \phi)$ averaged over $m = -\ell, \dots, \ell$ is equal to $1/(4\pi)$ for all θ, ϕ , and ℓ . For the case $\ell = 2$ (cf. Tab. I), Eq. (10) can be verified explicitly by averaging over the three-dimensional representation T_2^+ and the two-dimensional representation E^+ . The mass shifts for the S- and P-wave states are especially simple because these multiplets are not split apart into more than one cubic representation.

The sign of the finite volume mass shift can be explained in terms of the parity of the wave function. At infinite volume the tail of each bound state wave function must vanish at infinity. At finite volume, however, the bound state wave functions with even parity along a given axis can remain nonzero everywhere. Only the derivative needs to vanish at the boundary, and the kinetic energy is lowered by broadening of the wave function profile. On the other hand, a wave function with odd parity along a given axis must change sign across the boundary. In this

case the wave function profile is compressed and the kinetic energy is increased. We have illustrated both cases for a one-dimensional square well potential in Fig. 1.

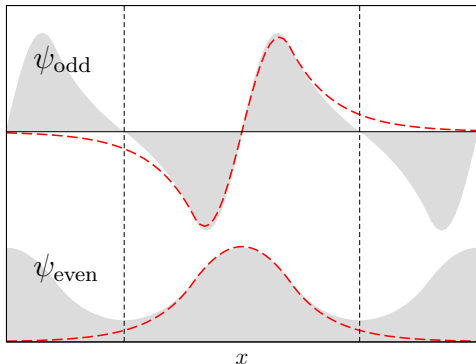


FIG. 1: (Color online) Wave functions with even (bottom) and odd parity (top) for a one-dimensional square well potential in a box with periodic boundary conditions. The dashed lines give the infinite volume solutions for comparison.

Comparison with numerical results. We test our predictions for the S-wave and P-wave mass shifts using numerical lattice calculations. In Fig. 2, we show the mass shifts obtained from numerically solving the Schrödinger equation for a lattice Gaussian potential

$$V(r) = -V_0 \exp(-r^2/(2R^2)) \quad (11)$$

with $R = 1$, $V_0 = 6$, and $\mu = 1$. All quantities are in lattice units. This potential does not have a finite range in a strict mathematical sense, but the range corrections can be entirely neglected. In order to compare the dependence on the box size L with the predicted behavior, we have plotted $\log(L \cdot |\Delta m_B|)$ against L (for S-waves Δm_B is negative). The expected linear dependence is clearly visible.

For comparison we have calculated mass shifts using three different methods. The crosses show the direct difference, Eq. (2), where we have used $L_\infty = 40$ to approximate the infinite volume solutions. The boxes were obtained from the overlap formula (3). The circles were calculated using discretized versions of (6) and (8), which we obtained by replacing $\exp(-\kappa r)/r$ with the lattice Green's function

$$G_\kappa(\mathbf{n}) = G\left(\mathbf{n}, -\frac{\kappa^2}{2\mu}\right) = \frac{1}{L^3} \sum_{\mathbf{q}} \frac{e^{-i\mathbf{q} \cdot \mathbf{n}}}{Q^2(\mathbf{q}) + \kappa^2}, \quad (12)$$

where $Q^2(\mathbf{q}) = 2 \sum_{i=1,2,3} (1 - \cos q_i)$. This Green's function is also used to calculate the asymptotic normalization γ from the lattice data. This incorporates the correct dispersion relation for our lattice model. Both the overlap and Green's function results were calculated using lattice wave functions from the $L_\infty = 40$ calculation.

All three results agree well for both the S-wave and P-wave. For small L there are visible deviations which

can be attributed to the $\mathcal{O}(e^{-\sqrt{2}\kappa L})$ -corrections as well as potential range effects. The inset in Fig. 2 shows this more clearly. There we plot the relative differences between the (logarithmic) direct results versus the overlap and Green's function data.

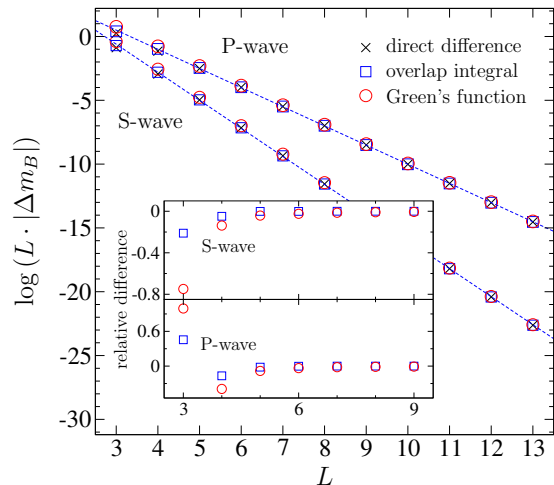


FIG. 2: (Color online) S- and P-wave mass shifts $\log(L \cdot |\Delta m_B|)$ as functions of the box size L (in lattice units). We show the results obtained from the direct difference Eq. (2) (crosses), evaluation of the overlap integral Eq. (3) (squares), and discretized versions of Eqs. (6), (8) (circles). The dashed lines are linear fits to the squares. In the inset, we show the relative difference between the direct results and the overlap (squares) and Green's function (circles) data.

When we perform a linear fit to the overlap integral data (dashed lines in Fig. 2) we obtain $\kappa = 2.198 \pm 0.005$, $|\gamma| = 11.5 \pm 0.2$ for the S-wave results; and $\kappa = 1.501 \pm 0.004$, $|\gamma| = 7.0 \pm 0.1$ for the P-wave results. The values for the asymptotic normalization are in good agreement with the results $|\gamma| \sim 11.5$ (S-wave) and $|\gamma| \sim 7.2$ (P-wave) that are obtained directly from the $L_\infty = 40$ data. Inserting the corresponding energy eigenvalues into the lattice dispersion relation

$$-\mu E_B = (1 - \cos(-i\kappa)) , \quad (13)$$

we find $\kappa \sim 2.211$ (S-wave) and $\kappa \sim 1.501$ (P-wave), again in quite good agreement with the fit results. The remaining small discrepancies can be attributed to the mixing with higher partial waves induced by the lattice discretization and the fact that we have not performed a continuum extrapolation to vanishing lattice spacing.

Summary and outlook. In this letter, we have derived an explicit formula for the mass shift of P- and D-wave bound states in a finite volume. We have compared our results with numerical calculations of the finite-volume dependence for a lattice Gaussian potential and found good agreement with predictions. For $\ell \geq 2$ the mass shift depends on the angular momentum projection m due to different representations of the cubic group. The

average mass shift in a multiplet with arbitrary angular momentum ℓ can be expressed in a simple way, and apart from the alternating sign it is independent of ℓ . Applications to nuclear halo systems such as ^{11}Be and molecular states in atomic and hadronic physics appear promising. Our study provides a general framework for future lattice studies of molecular states with angular momentum in systems with short-range interactions.

Finite-volume dependence can be used to probe the structure of a number of nuclei with conjectured alpha-cluster substructures [21–23]. Recently, there have been *ab initio* lattice calculations of the low-lying states of ^{12}C using effective field theory [24]. In particular, the energy for the spin-2 state of ^{12}C was calculated and found in agreement with the observed value of -87.72 MeV, just a few MeV below the triple-alpha threshold. It is not known how angular momentum is distributed in this state, and the study of finite volume effects may help to resolve this question.

Our results apply rigorously only to two-body systems. However, there is empirical evidence that Eq. (9) also gives the asymptotic L -dependence for three- and higher-body bound states at finite volume [25, 26]. In these cases the values of κ and γ are fitted empirically. We can show this explicitly using an extension of our Gaussian lattice model to three particle species. We take the particle masses to be equal, $m_1 = m_2 = m_3 = 2$, and consider Gaussian two-body potentials of the form (11) with the same range, $R = 2$, but different interaction strengths $V_0^{12} = 2.5$, $V_0^{23} = 3.0$, and $V_0^{31} = 3.5$ between the particles 12, 23, and 31, respectively.

In Fig. 3, we show the mass shifts as functions of the box size L (in lattice units). We show lattice results for the two lowest-lying trimer states with $J^P = 0^+$ and $J^P = 1^-$. All dimer states have less than half the binding energy of these trimers, which indicates that there is no underlying two-body molecular structure. As before we

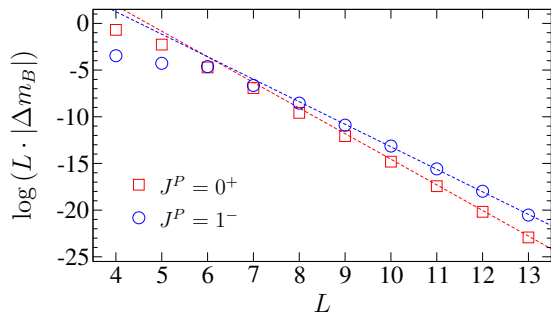


FIG. 3: (Color online) Trimer mass shifts $\log(-L \cdot |\Delta m_B|)$ as functions of the box size L (in lattice units). We show lattice results for the two lowest-lying trimer states with $J^P = 0^+$ (squares) and $J^P = 1^-$ (circles).

plot $\log(L \cdot |\Delta m_B|)$ against L . Analogous to the two-body case, we find that Δm_B for $J^P = 0^+$ is negative, while Δm_B for $J^P = 1^-$ is positive. We also find the same linear dependence for $\log(L \cdot |\Delta m_B|)$ at large L . Quite

interesting are the subleading corrections which are especially strong for $J^P = 1^-$ at smaller volumes. This may be due to competing finite volume corrections from negative S-wave and positive P-wave terms. These results point to a possible new application of finite volume corrections to probe the radial distribution of angular momentum in complicated bound state systems.

This research was supported in part by the DFG through SFB/TR 16 “Subnuclear structure of matter”, the BMBF under contract No. 06BN9006, and by the US Department of Energy under contract No. DE-FG02-03ER41260. S.K. was supported by the “Studienstiftung des deutschen Volkes” and by the Bonn-Cologne Graduate School of Physics and Astronomy.

-
- [1] D. Lee, Prog. Part. Nucl. Phys. **63** (2009) 117.
 - [2] A. Bazavov *et al.*, Rev. Mod. Phys. **82** (2010) 1349.
 - [3] S.R. Beane, W. Detmold, K. Orginos, and M.J. Savage, Prog. Part. Nucl. Phys. **66** (2011) 1.
 - [4] M. Lüscher, Commun. Math. Phys. **104** (1986) 177.
 - [5] S.R. Beane *et al.* (NPLQCD Collaboration), Phys. Rev. Lett. **106** (2011) 162001.
 - [6] K. Riisager, Rev. Mod. Phys. **66** (1994) 1105.
 - [7] S. Typel and G. Baur, Phys. Rev. Lett. **93** (2004) 142502.
 - [8] G. Rupak and R. Higa, Phys. Rev. Lett. **106** (2011) 222501.
 - [9] H.-W. Hammer and D.R. Phillips, Nucl. Phys. A **865** (2011) 17.
 - [10] C.A. Regal, C. Ticknor, J.L. Bohn, and D.S. Jin, Phys. Rev. Lett. **90** (2003) 053201.
 - [11] C.H. Schunck *et al.*, Phys. Rev. A **71** (2005) 045601.
 - [12] J.P. Gaebler, J.T. Stewart, J.L. Bohn, and D.S. Jin, Phys. Rev. Lett. **98** (2007) 200403.
 - [13] V.A. Novikov *et al.*, Phys. Rept. **41** (1978) 1.
 - [14] J. Bulava *et al.*, Phys. Rev. D **79** (2009) 034505.
 - [15] A. Matsuyama, T. Sato, T.-S.H. Lee, Phys. Rept. **439** (2007) 193.
 - [16] V. Bernard, M. Lage, U.-G. Meißner, and A. Rusetsky, JHEP **0808** (2008) 024.
 - [17] T. Luu and M.J. Savage, Phys. Rev. D **83** (2011) 114508.
 - [18] M. Lüscher, Nucl. Phys. B **354** (1991) 531.
 - [19] M. Abramowitz and I.A. Stegun, *Pocketbook of Mathematical Functions*, Verlag Harri Deutsch (1984).
 - [20] S. König, D. Lee, and H.-W. Hammer, *in preparation*.
 - [21] A. Tohsaki, H. Horiuchi, P. Schuck, and G. Röpke, Phys. Rev. Lett. **87** (2001) 192501.
 - [22] M. Chernykh, H. Feldmeier, T. Neff, P. von Neumann-Cosel, and A. Richter, Phys. Rev. Lett. **98** (2007) 032501.
 - [23] Y. Suzuki *et al.*, Phys. Lett. B **659** (2008) 160.
 - [24] E. Epelbaum, H. Krebs, D. Lee, and U.-G. Meißner, Phys. Rev. Lett. **104** (2010) 142501; Phys. Rev. Lett. **106** (2011) 192501.
 - [25] E. Epelbaum, H. Krebs, D. Lee, and U.-G. Meißner, Eur. Phys. J. A **41** (2009) 125.
 - [26] S. Kreuzer and H.-W. Hammer, Phys. Lett. B **673** (2009) 260; Eur. Phys. J. A **43** (2010) 229; Phys. Lett. B **694** (2011) 424.